Wiley
Journal of Engineering
Volume 2025, Article ID 2225558, 14 pages
https://doi.org/10.1155/je/2225558

WILEY

Research Article

Efficiency of Bagasse Ash Incorporated With Limestone Calcined Clay Cement on Improvement of Geotechnical Properties of Black Cotton Soils: A Cleaner Approach

Horris K. Nangulama[1] **and Witness Kuotcha**[2]

[1]*Department of Mining Engineering, Malawi University of Business and Applied Sciences, Blantyre, Malawi*
[2]*School of Built Environment, Malawi University of Business and Applied Sciences, Blantyre, Malawi*

Correspondence should be addressed to Horris K. Nangulama; hnangulama@mubas.ac.mw

Received 28 April 2025; Revised 14 August 2025; Accepted 15 September 2025

Academic Editor: Claudio Mazzotti

This study is aimed at investigating the effect of sugarcane bagasse ash (BA) incorporated with limestone calcined clay cement (LC^3) as potential alternative from technical, ecological and economic perspectives of black cotton soil (BCS) stabilisation. BA incorporating LC^3 material was added to BCS having high swell degree, in mix proportions of 0%–18%. Series of laboratory tests were conducted in terms of free swell index (FSI), compaction, unconfined compressive strength (UCS), California bearing ratio (CBR) and shear strength engineering properties. Besides, microstructure changes were evaluated in terms of pore size distribution (PSD), x-ray diffraction (XRD) and scanning electron microscope (SEM) to analyse factors responsible for performance improvement of stabilised BCS. Results indicated that BA incorporating LC^3 binder stabilisation completely eradicated swelling behaviour and improved strength performance of BCS. FSI reduced by 71.8%, UCS increased and CBR performance attained 80% threshold, complying with requirements for foundation soil road applications. Shear strength and cohesion increased with increase in binder content and curing period. Performance of 12% BA incorporating LC^3 binder additive content to BCS was found to have highest internal friction angle. Microstructure evaluations showed that calcium aluminosilicate hydrates (CASHs) are prime cementitious products formed behind stabilised BCS. Analysis pertaining to carbon footprint and cost indicated that BA incorporating LC^3 binder is a more cleaner and cost-effective construction material. This study promotes application of BA incorporating LC^3 binder technique for BCS treatment in pursuit to mitigate current climate change emergency and reduce high cost encountered during routine BCS stabilisation practice.

Keywords: black cotton soil stabilisation; cleaner construction; cost-effective construction; performance enhancement; road construction

1. Introduction

Black cotton soil (BCS) is understood for its challenging high-volume change and low strength, which induce premature failures of road infrastructures [1–8]. Due to limited land space availability and rapid population growth, inescapably, many road infrastructures are still built on BCS [4–7]. Presently, chemical treatment using OPC binder is commonly used to stabilise BCS [3, 8]. But OPC is an energy-intense binder with lofty carbon anthropogenic emissions [9–15]. The production of OPC not only generates a substantial amount of carbon footprint but also consumes a large quantity of nonrenewable resources [9–12]. For example, 1.5 ton equivalent raw material is demanded for about 1.0 ton production of OPC, from which 1.0 ton of carbon dioxide (CO_2) is extricated into the environment [11, 13]. Besides, whenever mass BCS treatment is required, the consumption of OPC is relatively high and costly [2–6]. Thus, it is of vital importance and significant engineering magnitude to search for new alternative materials in place of OPC for use in BCS stabilisation practice.

In recent years, blended cements with comparable strength performance to OPC have been developed and used as supplementary cementitious materials (SCMs) [16–19].

Many research works have indicated that about 30% of SCMs such as fly ash, ground granulated blast-furnace slag (GGBS), eucalyptus ash, bentonite and silica fume–based geopolymers are integrated as additives in cement [20–25]. Geopolymer-based materials have high potential to reduce carbon emissions and resource consumption [20, 25]. Substituting OPC with geopolymer-based materials has suitably enhanced the properties of stabilised BCS and has decreased both environmental effects and high BCS treatment costs [1, 20, 21]. However, in some countries, such as Malawi, which do not rely on fossil fuels to generate power, the availability of GGBS and the quality of fly ash are the main drawbacks for their employment in the development of cement [26]. Besides, the feasibility of geopolymer-based materials is noticeable in the medium to long term [20, 25]. Broader use of geopolymer-based materials such as fly ash and GGBS in BCS stabilisation encounters some challenges such as restrained accessibility, minimal reactivity and their various effects on the performance of treated BCS [1, 3, 21]. As the geotechnical construction sector continues to grow rapidly, the employment of new and locally available innovative techniques for BCS treatment is significantly important to address the carbon footprint and high BCS stabilisation costs for a more sustainable future.

Bagasse ash (BA) shows prospects as a partial replacement of OPC in BCS stabilisation, although its effectiveness is limited [4, 6]. The sugar-producing industry may burn bagasse waste, which is obtained from sugarcane after extracting juice as fuel in a combined generator to produce electricity, and BA becomes the final waste during that process [27]. A thousand kilogrammes of bagasse waste may yield about 30–45 kg of BA [27]. Recent research works have revealed the use of BA in mortars as a sustainable way of its disposal [28, 29]. Several studies indicate that BA-modified mortars can be used in the products of cement, owing to their significant physicochemical properties [30–33]. Wu et al. [27] carried out research and replaced OPC in the range of 0%–30% with BA to produce concrete. Their findings showed that composites with 18% BA depicted good workability and resistance properties. Serker et al. [30] investigated the compressive strength of modified concrete with 0%–50% of BA. Bahurudeen et al. [32] showed the feasibility of BA as an ingredient in minimising composites of cement. These studies justify the practicality of the employment of BA as a cementitious material. In terms of BCS treatment, the adoption of BA as a stabilising material has been broadly reported by several studies [4, 6, 33]. However, the sole examination of BA to fulfil serviceability and strength criteria of treated BCS implies that BA alone is not suitable for stabilising BCS subgrades relevant to pavement construction [4, 33]. Several studies assessed the incorporation of additive materials such as fly ash, lime and coir fibres to BA for stabilisation of BCS [1, 4, 33]. These studies discovered that such incorporations curtailed the plasticity index (PI) of the treated BCS, although the increase in the California bearing ratio (CBR) of treated BCS was insignificant. Incorporating BA with OPC improved unconfined compressive strength (UCS) of BCS and managed BA disposal concerns through BA waste reduction [34, 35]. The application of BA incorporating OPC exhibited a significant decline in PI, free swell index (FSI) potential, maximum dry density (MDD) and an increase in optimum moisture content (OMC) of treated BCS [34]. Himani et al. [6] examined the reduction in heave and swell pressure due to the addition of BA incorporating OPC content in BCS samples, and significant improvements of treated BCS samples were reported. These previous studies verify the capacity of BA incorporating OPC on the improvement of the engineering behaviour of BCS. However, the utilisation of OPC as an incorporating material to BA might raise carbon footprint environmental concerns and significantly increase the BCS stabilisation costs compared to the related benefits [9–13].

Limestone calcined clay cement (LC^3) is one of the new types of SCMs that can minimise CO_2 emissions by at least 40% in comparison to OPC [36–38]. LC^3 comprises three main components, namely, limestone (LS), calcined clay (CC) and cement clinker (CL) [37, 39]. Its mechanical and strength performances largely depend on the mix proportions of its main components [40]. For example, Diaz et al. [36] reported that the filling effect of LS and high pozzolanic reactivity of CC are significant in the enhancement of mechanical and durability characteristics of LC^3-based composites. Besides, CC, which is obtained after calcining clay, is globally distributed and rich in reserves [40], making its availability sustainable [38]. Moreover, LC^3 manufacture does not require new technologies, making it inexpensive and easy to introduce to the construction sector [26]. Compared to OPC, the LC^3 notable features lie in being able to decrease the consumption of cement CL by almost 50% whilst facilitating the dense rheological formation just as OPC, leading to enhanced mechanical strength and improved durability [41, 42]. Several studies have been published so far with regard to the use of LC^3 as a substitute for OPC. For example, Mohamed et al. [41] analysed the impacts of CC on the performance of LC^3 concrete. Kafodya et al. [26] provided valuable insights into LC^3 and its influence on hydration activities. Some recent research works of Wang et al. [43] and Reddy et al. [44], respectively, centred on the stabilisation of zinc and radioactive borate-contaminated soils with LC^3 and demonstrated its capacity to alter the properties of treated soils through hydration reactions. Generally, the previous studies demonstrate the feasibility of LC^3 as a great performance reliable cement. Just as Ijaz et al. [40], Sharma et al. [42] showed that LC^3 can be applied just as OPC and does not require special training. Thus, BA can be incorporated with LC^3 in the same manner that BA is incorporated with OPC [45, 46]. Overall, a combined utilisation of BA and LC^3 as cementitious material has significant potential to meet the extensive amounts of materials demanded by the cement industry for routine BCS stabilisation practice to ensure green, cost-effective, sustainable and resilient pavement constructions.

Although BA and LC^3 have demonstrated substantial potential to be utilised in concrete and in BCS stabilisation practice, there are enormous gaps in literature on the optimal quantities of BA incorporating LC^3 required for use as SCMs for BCS treatment. The effectiveness of BA incorporating LC^3 in BCS stabilisation is still not known. The

TABLE 1: Engineering properties of BA, LC^3, OPC and BCS.

Chemical properties	SiO_2 (%)	Al_2O_3 (%)	Fe_2O_3 (%)	CaO (%)	Na_2O (%)	SO_3 (%)	MgO (%)	K_2O (%)	LOI (%)
BA	64.35	4.92	4.12	10.23	0.61	1.85	3.25	2.97	2.11
LC^3	25.16	4.01	2.24	61.37	0.14	2.44	1.60	0.43	1.55
OPC	21.83	4.47	2.68	59.81	0.32	2.28	1.42	0.51	0.98
BCS	66.12	13.15	7.64	0.59	2.79	1.01	6.51	1.36	6.52

Physical properties of BCS	Test method	Mean value
Natural moisture content	ASTM D2216 [47]	36.71%
Specific gravity	ASTM D854 [48]	2.35
Plasticity	ASTM D4318 [49]	—
Liquid limit	—	81.02%
Plastic limit	—	32.77%
Plasticity index	—	48.25%
Particle size distribution	ASTM D6913 [50]	—
Clay	—	62.48%
Silt	—	27.85%
Sand	—	9.67%
Gravel	—	0.00%

fundamental stabilisation mechanism through which BA incorporating LC^3 can interact with minerals present in BCS to enhance its properties has not been explored or established. This study narrows these critical knowledge gaps to show the potential and suitability of BA incorporating LC^3 in enhancing the engineering performance of treated BCS. The works in this study explore this new combination of BA with LC^3 by varying additive content of BA incorporating LC^3 to BCS. The use of BA and LC^3 is critical to uncover their combined influence on treated BCS performance. This is significant to geotechnical construction sector in terms of providing clues regarding the best BA incorporating LC^3 content for stabilisation of BCS from performance and sustainability perspectives. Thus, this study advances the high value and safe use of BA and LC^3 materials. The study further promotes the use of BA incorporating LC^3 technique for routine BCS stabilisation practice relevant to road pavement applications, aligning with efforts to address climate change and reduce infrastructure development costs.

2. Materials and Methods

2.1. Materials. BA, LC^3 and BCS are primary materials adopted in this study. All materials were collected from Shire Valley in Malawi, which is geographically located at an elevated range of 34–106 m and between 34° 15′ E–35° 16′ E longitudes as well as between 15° 29′ S–16° 46′ S latitudes.

BA was obtained from ILLOVO Sugar Company during boiler cleaning process. It was collected at 530°C boiler temperature in consistent with previous studies [6, 28]. Then, it was cooled, manually grinded to powder and sieved using 300 μm sieves to remove undesirable materials [27]. Its physical properties were measured, and results indicated that this BA has a specific gravity of 2.52, a particle size (d_{50}) of 26.97 μm and a Blaine surface area of 513 m^2/kg and it was black in colour. For pozzolanic reactivity of this BA, chemical properties were measured using Xenemetrix X-Calibur x-ray fluorescence (XRF) spectrometry, and results are portrayed in Table 1. Based on ASTM C618 [51] specification, a natural pozzolana with at least 70% total percentage of SiO_2, Al_2O_3 and Fe_2O_3 is classified as Class F pozzolanic material. Hence, this BA belongs to Class F pozzolana [51].

To prepare LC^3, collected kaolinite clay was calcined for 30 min at 800°C ± 10°C temperature in a furnace to produce CC. This temperature is the dehydroxylation top range of the kaolinite clay mineral group [38], whereas 30 min is the shortest period that ensures complete structural breakup of the kaolinite clay mineral [38]. LS and gypsum (Gyp) were collected and separately grinded to produce a fine powder. CL was acquired from a local Shayona Portland cement manufacturing (SPCM) distributor. Only volumes of materials of CC, LS, Gyp and CL, finer than 75 μm, were used for preparing LC^3 material. LC^3 was prepared with 30% CC, 15% LS, 5% Gyp and 50% CL, in agreement with previous studies [37–41]. Besides, OPC classified as CEM I: 42.5 N, conforming to ASTM C150 [52] specification, was used. OPC was used as a control for comparison purposes. Loss on ignition (LOI) and mineralogical compositions of both prepared LC^3 and OPC were determined by means of XRF analysis, and results are tabulated in Table 1.

BCS was collected at 1.5 m depth to avoid foreign matters [1, 2]. Then, it was oven-dried for 24 h at 110°C to completely dry it up [4]. It was then sieved using 2.0 mm sieves to prepare even specimens [2, 3]. Its engineering properties were measured, and the results are given in Table 1. Results in Table 1 comparably dive within the scope measured for BCS by similar studies [1–6]. Based on Table 1 measurements, this BCS was classified as clayey silt and

was identified as A-7-6 with regard to the AASHTO soil classification system. Thus, this BCS is much problematic for application without treatment as foundation material for road pavement constructions [1–8].

2.2. Methods. BA was incorporated with LC^3 in the mix ratio of 3:2, in agreement with previous studies [53, 54]. To optimise and validate the effectiveness of the adopted 3:2 BA incorporating LC^3 mix ratio, its performance was investigated in terms of compressive strength properties. The obtained results were compared with other different mix ratios of 3:1 and 3:3, which were randomly selected to provide a base for comparison purposes. For each mix proportion, the water-to-cement (w/c) ratio was kept at 0.45, 0.5 and 0.6, and the properties of each mixture at each w/c ratio were separately investigated. Concrete tubes with sizes of 150.0 mm were prepared as per BS EN 12390 [55] recommendation. Three test samples were cured for 28 days and kept in a room under standard curing conditions (95% relative humidity and 24°C temperature). The compressive strength test was conducted as per BS EN 12390 [55] specification, and the average values of the measured results are shown in Figure 1. Maximum compressive strengths at 3:1, 3:2 and 3:3 mix ratios were 28.6, 31.7 and 29.3 MPa at 0.45, 0.5 and 0.6 w/c ratios, respectively. With respect to BS EN 197 [56] and BS EN 413 [57] specifications, the 3:2 BA incorporating LC^3 mix ratio satisfied the allowable 30 MPa minimum required compressive strength limit for concrete cubes at the standard curing period of 28 days.

Effectiveness of 3:2 BA incorporating LC^3 mixture on BCS stabilisation was investigated in mix proportions of 0%–18% on treated BCS, in terms of FSI, compaction, UCS, CBR and shear strength properties for specimens cured for 7, 14 and 28 days at standard 24°C room temperature and 95% relative humidity. Besides, factors responsible for strength improvement of stabilised BCS were evaluated in terms of pore size distribution (PSD), x-ray diffraction (XRD) and scanning electron microscope (SEM) analyses for samples cured at standard 28 days. Moreover, OPC binder was incorporated into the results at 7% content to provide a base for comparison and optimisation purposes. The 7% OPC binder content was selected as optimum content for effective BCS stabilisation based on previous studies [3, 8].

BCS specimens for various tests were prepared using 600 kN-m/m^3 standard compaction effort at 95% MDD. 2.5% moisture content was added in surplus of OMC to grapple with inherent losses in moisture content and to render cement hydration. A parallel technique is adopted for in situ BCS stabilisation methods [2]. Standard proctor compaction test was performed following the procedure outlined in ASTM D698 [58] specification. FSI test was performed on prepared specimens in accordance with ASTM D4829 [59] specification. Prior to the FSI test, specimens were oven-dried for 24 h at 105°C to further dry them up [8]. After drying, specimens were poured slowly into 1000 mm^3 measuring jars which were filled with distilled water. Then specimen-filled jars were gently shaken with a string glass rod to remove any entrapped air [8]. After shaking, specimen-filled jars were left for 24 h. After 24 h, the volume

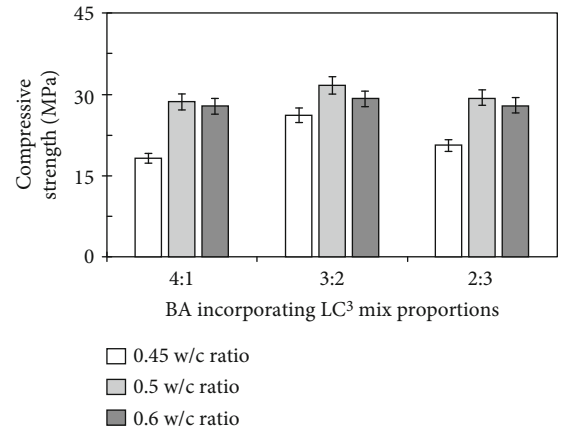

Figure 1: Compressive strength comparative study between different mix ratios of BA incorporated with LC^3 additive contents.

TABLE 2: Classification of potential FSI of soils.

FSI (%)	Swelling potential
> 130	Very high
91–130	High
41–90	Medium
21–40	Low
0–20	Very low

of the jars was recorded, and FSI was determined as the volume increase of each specimen expressed as a percentage of its initial volume. Outcomes were interpreted with respect to Table 2, which provides classification of FSI of soils based on ASTM D4829 [59] classifications. The UCS test was conducted on compacted specimens in accordance with ASTM D2166 [60] specification. Compacted specimens at their respective MDD and OMC were extruded from moulds having a diameter of about 50 mm and height of about 100 mm. Specimens were then sealed and cured for 7, 14 and 28 days prior to the UCS test. A strain rate of 1.0 mm/min was used for the UCS test, and UCS was calculated as the maximum load attained per unit area. CBR test was performed on compacted specimens as per ASTM D1883 [61] specification. Specimens for CBR test were prepared at OMC and MDD. CBR test was calculated as the percentage of measured load against standard load. CBR specimens were tested in soaked conditions to portray the worst-case scenario where treated BCS specimens may be under flooding, as is the most common case with Shire Valley in Malawi. Consolidated-drained (CD) direct shear test was performed on prepared specimens at MDD and OMC compaction parameters. After desired curing periods, specimens for CD direct shear test were subjected to four different confining pressures of 50, 150, 300 and 450 kPa, and the CD direct shear test was performed as per ASTM D3080 [62] specification using a ZJ-1B type electrical strain-controlled direct shear apparatus. For PSD, XRD and SEM measurements, crushed UCS specimens were collected, cast in ⌀33 × 54 mm plastic-sealed containers, then cured at 24°C standard temperature for 28 days. After

TABLE 3: Test programme of untreated and treated BCS.

Specimens		Test method		Test set
Untreated BCS		Swelling potential	FSI	1
		Compaction	Standard proctor	1
		Unconfined strength	UCS	1
		Bearing ratio	CBR	1
		PSD	MIP	1
		Mineralogy	XRD	1
		Microstructure	SEM	1
Treated BCS	Treated with 3%, 6%, 9%, 12% and 18% BA incorporating LC^3 binder content and 7% OPC binder content for comparison purposes	Swelling potential	FSI	6
		Compaction	Standard proctor	6
		Unconfined strength	UCS	6
		Bearing ratio	CBR	6
		Shear strength	CD	6
		PSD	MIP	6
		Mineralogy	XRD	6
	Treated with 18% BA incorporating LC^3 content	Microstructure	SEM	1
Total test sets				50

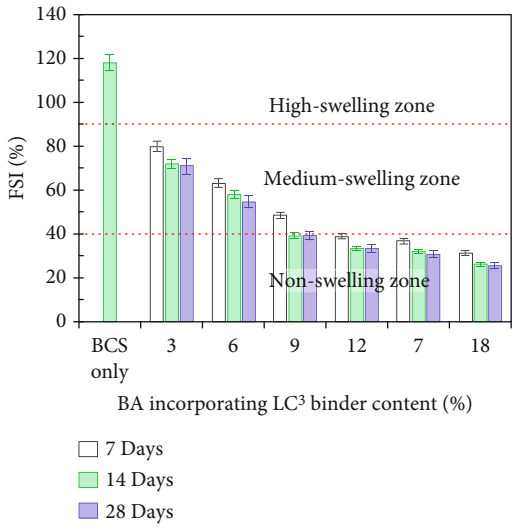

FIGURE 2: FSI variations of treated BCS at various binder contents and curing ages.

curing, specimens were broken into smaller pieces and submerged in ethanol (anhydrous) to cease hydration. For every 24 h, ethanol was replaced. After 48 h, specimens were placed in a vacuum dryer to dry them to a constant mass. Specimens were then grinded to powder following drying and sieved using a 75 μm sieve. PSD was conducted using mercury intrusion porosimetry (MIP-2000X) method, XRD was performed using D8-advanced powder diffractometry (D8-APD) technique and SEM was conducted using MIRA3 TESCAN (Hitachi S-520 SEM) analysis. Overall, a total of 50 test sets were conducted as outlined in Table 3, and for each test set (except for PSD, XRD and SEM, which only involved one test set), two more test sets were performed, and the average was considered for interpretations.

3. Results and Discussions

3.1. FSI Properties. Figure 2 shows the measured FSI of untreated and treated BCS specimens. This BCS has high swelling properties considering its measured FSI of 118.07% [3, 5]. Such a great swell degree is challenging and may lead to premature failures of road structures built on it [1, 2, 7]. Conversely, with the addition of BA incorporating LC^3 binder content, FSI was reduced significantly. Similar performance in FSI can also be observed for OPC binder-treated BCS incorporated in this study for comparison purposes. For example, at 12% BA incorporating LC^3 binder content, the FSI of treated BCS reduced from 118.07% to 33.29%, considering samples cured for 28 days. Hence, transforming the BCS from a high swell zone to a nonswell zone, with an overall reduction of about 71.8%. A similar observation can also be noticed for 7% OPC binder-treated BCS, with an overall reduction of about 72.1% at 28 curing days. This significant enhancement in FSI of treated BCS can be attributed to the potential ionisation of BCS and the stabilising binder matrix, leading to cementation behaviour [2–6]. Furthermore, LC^3 has higher content of CaO, whilst BA has higher SiO_2 and Al_2O_3 contents (Table 1). The combination of these minerals and water may have induced a pozzolanic reaction, resulting in the development of cementitious hydration products such as calcium aluminosilicate hydrate (CASH) gels (Table 4), which filled the voids of BCS particles and cemented BCS particles, developing a denser microstructure, altering physical and mechanical characteristics and ultimately resulting in swelling reduction [5–8].

3.2. Compaction Properties. Figure 3 depicts variations in compaction parameters, such as OMC and MDD, with an increase in BA incorporating LC^3 binder content addition to BCS. Results show that OMC and MDD differed with BA incorporating LC^3 binder content increase from 0% to

TABLE 4: Controlling chemical processes.

Reaction	Chemical process	Products
Hydration	$CaO + H_2O \rightarrow Ca(OH)_2$	Calcium hydrate (CH)
Pozzolanic	$Ca(OH)_2 + SiO_2 \rightarrow CSH$	Calcium silica hydrate (CSH)
Pozzolanic	$Ca(OH)_2 + Al_2O_3 \rightarrow CAH$	Calcium alumina hydrate (CAH)
Pozzolanic	$Ca(OH)_2 + Al_2O_3 + SiO_2 \rightarrow CASH$	Calcium aluminosilicate hydrate (CASH)
Dissolution	$Ca(OH)_2 \rightarrow Ca^{2+} + 2OH^-$	Calcium and hydroxide ions (Ca^{2+} and OH^-)

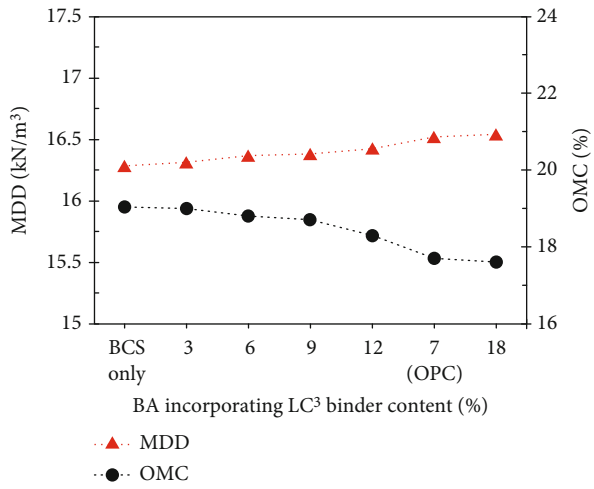

FIGURE 3: MDD and OMC variations of treated BCS at various binder contents.

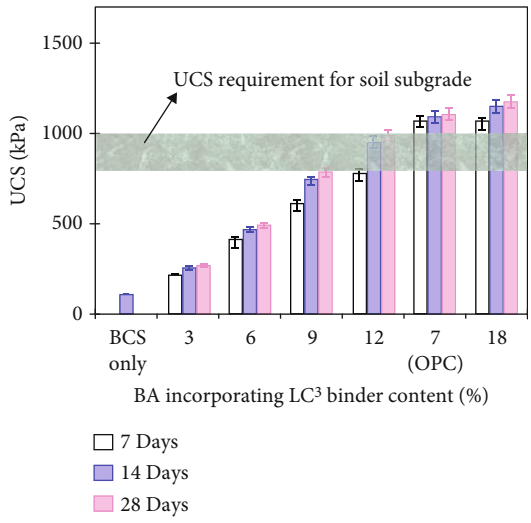

FIGURE 4: UCS variations of treated BCS at various binder contents and curing ages.

18%. For example, at lower content (i.e. 3%), variations in OMC and MDD are negligible, whilst at higher content (i.e. 18%), OMC reduces, and MDD increases significantly. Moreover, for comparison purposes, the effect of OPC binder at 7% content was incorporated. Results revealed that 7% content of OPC binder prompted a similar kind of increase in MDD. For instance, compared to untreated

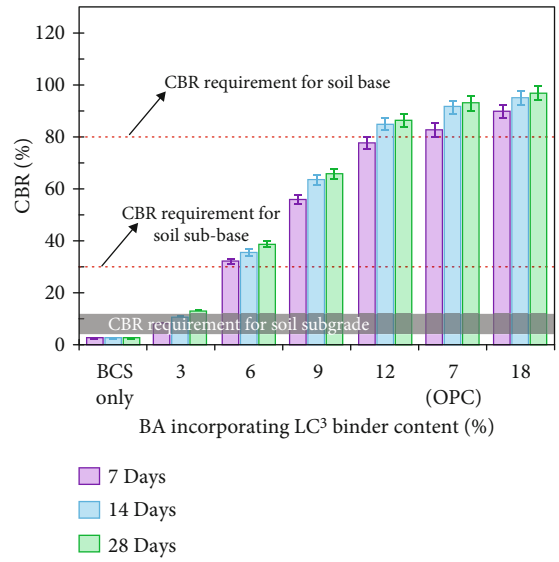

FIGURE 5: CBR variations of treated BCS at various binder contents and curing ages.

BCS, the MDD of treated BCS with 12% BA incorporating LC^3 binder and 7% OPC binder increased by about 1.15% and 2.06%, respectively. Overall, the improvement in OMC and MDD with binder additive contents was attributed to flocculation and agglomeration between BCS particles due to the pozzolanic reaction (Table 4). This phenomenon wrapped together the BCS particles, leading to improved OMC and MDD values of treated BCS, as previously argued [20, 21].

3.3. UCS Properties. Measured UCS of untreated and treated BCS at various contents of BA incorporating LC^3 binder is presented in Figure 4. For untreated BCS, UCS was determined to be relatively low (about 109.2 kPa). With increasing BA incorporating LC^3 binder content, a notable UCS increase was observed along with curing age. At lower content, there was a little UCS increase at all curing ages. To illustrate, at 3% BA incorporating LC^3 binder content, UCS on the 28th day only increased by about 1.97 times untreated BCS. However, at higher content, there was a notable increase in UCS values. For example, at 18% BA incorporating LC^3 binder content, UCS on the 28th day significantly increased by about 10.76 times untreated BCS. In addition, UCS of BCS treated with 7% OPC binder content was embodied into the results. Overall, outcomes were

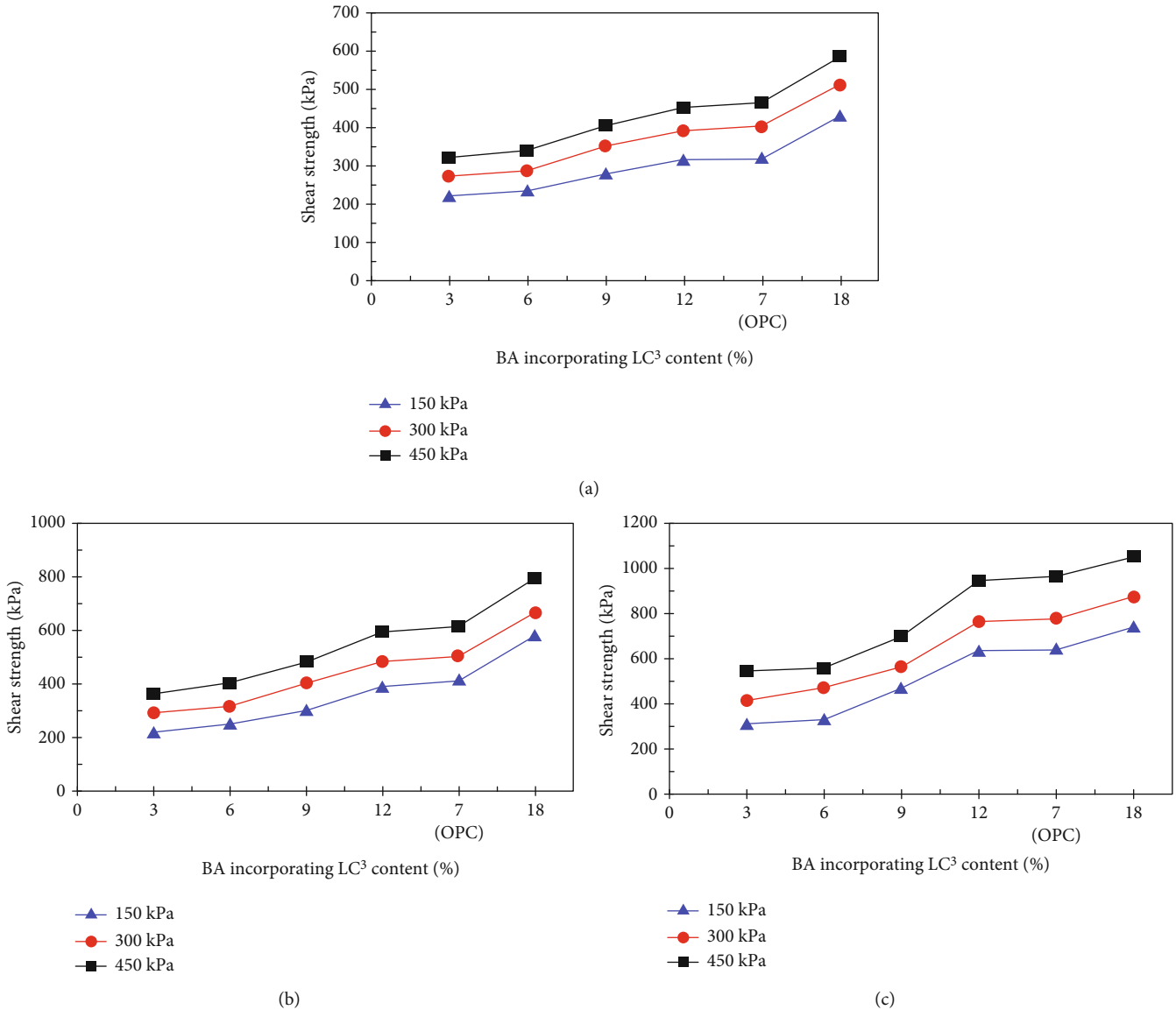

Figure 6: Variations in shear strength at various curing ages: (a) 7, (b) 14 and (c) 28 days.

determined to be comparably similar. For example, at 12% BA incorporating LC^3 binder content and 7% OPC binder content, UCS values on the 28th day have been increased by 9.04 and 10.14 times untreated BCS, respectively. Whereas at 6% and 9% BA incorporating LC^3 binder contents, UCS on the 28th day was, respectively, found to be 4.51 and 7.16 times untreated BCS. Moreover, it is essential to observe from Figure 4 that after 14 curing days, the increase in UCS is minimal, implying that major reactions were completed within 14 days. Besides, the area that is shaded in Figure 4 portrays that soil subgrade or subbase for low volume roads should meet UCS requirement of 800–1000 kPa based on MMWT [63] soil test method. Results revealed that BCS treated with 12% BA incorporating LC^3 binder content satisfied the allowable requirement at 14 and 28 curing days, whereas 18% BA incorporating LC^3 binder content satisfied the requirement at all curing ages. Overall, the obtained strength improvement results were attributed to the cohesion of BCS particles caused by pozzolanic reaction due to the mixing of BCS, BA incorporating LC^3 binder and water. This mixing resulted in flocculation and agglomeration between BCS particles, leading to the development of a significant number of cementitious hydration products, which wrapped together BCS particles and eventually resulted in the strength enhancement of treated BCS. Similar conclusions were also drawn from similar experiments [33–35].

3.4. CBR Properties. Figure 5 portrays CBR results of untreated and treated BCS specimens. CBR was noticed to increase with an increase in additive content of BA incorporating LC^3 binder to BCS. The highest recorded CBR was 98.7% at 18% BA incorporating LC^3 binder content addition to BCS, considering 28 curing days. The increase in CBR was justified by mixing of BCS, BA incorporating LC^3 binder and water. This mixture led to hydration reaction and

development of $Ca(OH)_2$ and CASH gels. Eventually, reactive BCS particles reacted with $Ca(OH)_2$. This resulted in the development of a significant number of products, such as Ca^{2+} and OH^-, which wrapped BCS particle surfaces and created a network structure, leading to CBR enhancement. Besides, CBR of OPC-treated BCS at 7% content was also integrated. Outcomes were found to be comparably similar. To illustrate, at 7% OPC binder content and 12% BA incorporating LC^3 binder content, CBR was almost identical with an increase of about 38.54 and 36.79 times untreated BCS, respectively, considering 28 days of curing, satisfying required minimum CBR thresholds of 5%–11%, 30% and 80% for subgrade, subbase and base-course road pavement structural materials, respectively [63–65].

3.5. Shear Strength Properties. Figure 6 shows the shear strength of treated BCS under different vertical pressures of 150, 300 and 450 kPa. As observed in Figure 6, shear strength increased with an increase in binder content, vertical pressure and curing age. To illustrate, the shear strength of 18% treated BCS cured for 7 days under 450 kPa vertical pressure was 82.81% higher than that of 3% treated BCS. Shear strength increased by about 36.05% with an increase in vertical pressure from 150 to 450 kPa at 7 days of curing. Kasama et al. [66] concluded that an increase in vertical pressure results in treated swelling soil undergoing significant fragmentation of particles, leading to denser configuration and spatial reorganisation, enabling treated soil to withstand increased vertical pressures. In regard to the influence of curing age, shear strength increased by about 35.04% from 7 to 14 days of curing, considering 18% BA incorporating LC^3 binder additive content. Further increase in shear strength was also noticed with a further increase in curing age (i.e. at 28 curing days). This phenomenon was attributed to different curing ages, with low age inhibiting the rate of hydration reaction, as also concluded by Calik and Sadoglu [67] and Kang et al. [68]. Besides, the shear strength of BA incorporating LC^3 binder-treated BCS was comparably equal to that of OPC binder-treated BCS. To exemplify, the shear strength at 12% BA incorporating LC^3 binder content was 941.38 kPa and that at 7% OPC binder-treated BCS was 958.72 kPa, considering 28 days of curing. Overall, the increase in shear strength of treated BCS was justified by the formation of hydration products, resulting in improvement of the internal structural matrix and compactness, hence, shear strength enhancement [20, 33]. This discovery is consistent with previous research works [66–68].

Besides, Figure 7 provides the relationship between BA incorporating LC^3 binder content and the cohesion of treated BCS. It can be seen that there is an increase in cohesion with an increase in BA incorporating LC^3 binder content and curing period. Overall, the increase in cohesion was primarily related to the continuous effect of hydration products on BCS pores, in which the development and accumulation of hydration products on BCS pores were progressively impacted by BA incorporating LC^3 binder content and curing period. Adhesion between treated BCS particles was essentially strengthened; thus, the cohesion of BA incorporating LC^3 binder-treated BCS was further improved. This

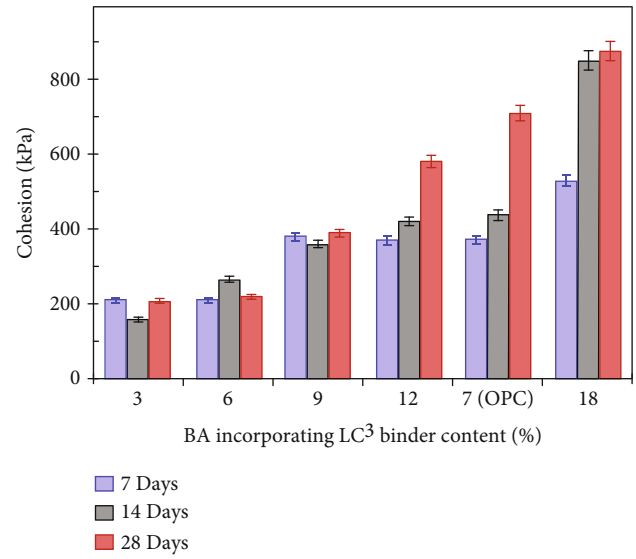

Figure 7: Variations in cohesion of treated BCS at various contents and curing ages.

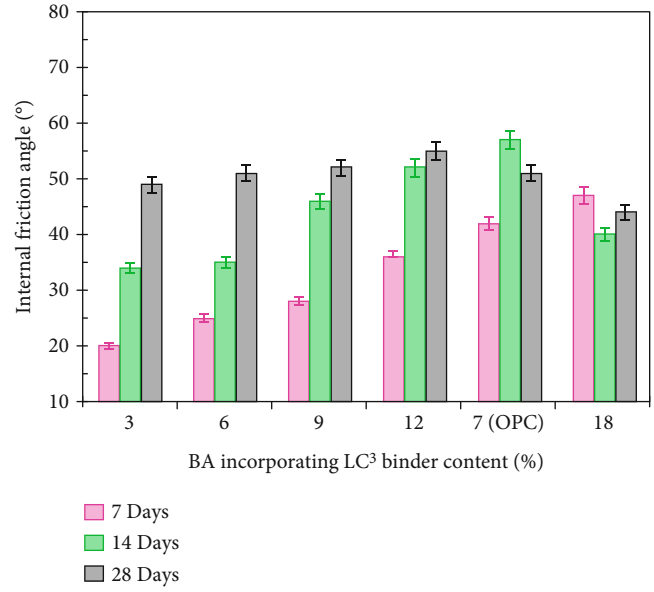

Figure 8: Variations in internal friction angle of treated BCS at various contents and curing ages.

phenomenon can also be depicted in Figure 8 which portrays the relationship between BA incorporating LC^3 binder content and the internal friction angle of treated BCS at different curing periods. It can be seen that the internal friction angle varies with an increase in BA incorporating LC^3 binder content. To illustrate, at 3%, 6% and 9% BA incorporating LC^3 binder contents, there is an increase and decrease in behaviour in the internal friction angle of treated BCS at all curing periods. This is in comparison with 12% and 18% BA incorporating LC^3 binder contents, where a continuous increase in internal friction angle was observed. This demonstrates that in order to get the highest internal friction angle, an optimum BA incorporating LC^3 binder content

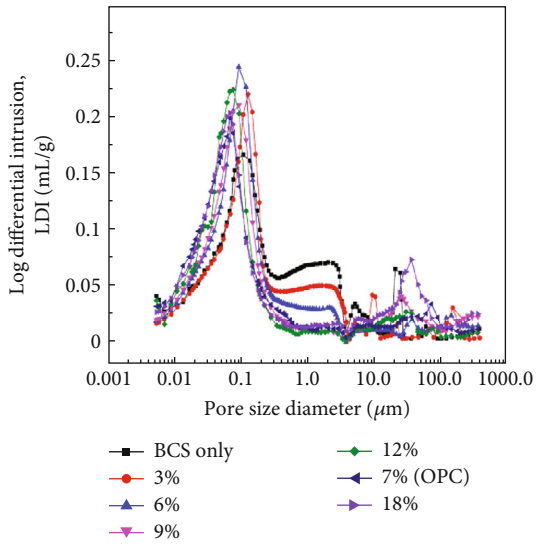

Figure 9: Variations in PSD at various binder contents for specimens cured at 28 days.

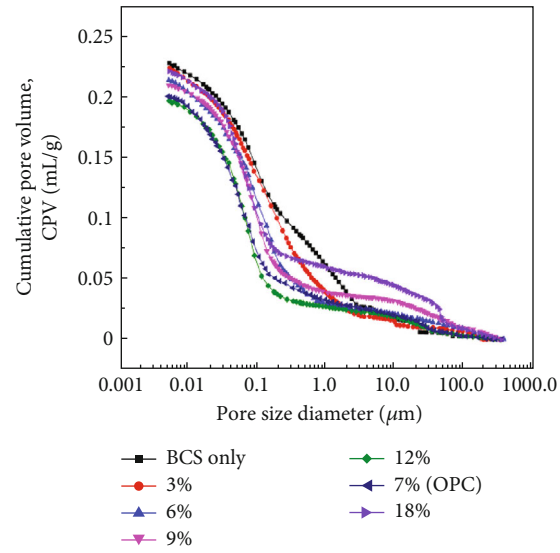

Figure 10: Variations in CPV at various binder contents for specimens cured at 28 days.

should be used. Thus, the optimum BA incorporating LC^3 binder for BCS treatment in this study ranged from 12% content. This finding was justified by the intense hydration reaction due to BA incorporating LC^3 binder content and curing period, leading to the formation of more hydration products which effectively filled large pores, hence, the internal friction angle improvement and strength enhancement.

3.6. PSD, XRD and SEM Properties. Figure 9 shows PSD results of untreated and treated BCS with BA incorporating LC^3 binder for specimens cured at 28 days. Untreated BCS exhibited a bimodal curve type of PSD, with the opening mode characterised by about 0.01–0.30 μm pore size range accompanied by a subsequent range of about 0.30–4.0 μm pore sizes. This initial mode of smaller diameter was justified by intra-assemblage pore space, dominating the BCS matrix, whereas the later mode with a bigger diameter was attributed to interassemblage pore spaces. With the addition of binder content, the PSD of untreated BCS happens to tilt to the left in support of smaller pore size diameter. To illustrate, at 6% BA incorporating LC^3 binder content, the pore size diameter peak within the 0.30–4.0 μm range falls and seems to lessen and modify towards a unimodal curve type from bimodal type due to increased formation of finer micropores (i.e. 0.01–0.10 μm). Whereas at 18% BA incorporating LC^3 binder content, pore sizes within the 0.30–4.0 μm range vanished due to a continued increase in smaller pore sizes. For instance, the shifting of the 0.10 μm peak to the 0.05 μm peak highlighted porous structure refinement, leading to a denser structure formation with notable enhancement compared to untreated BCS. Besides, the PSD at 7% OPC binder-treated BCS was measured to be comparably parallel to that of 12% BA incorporating LC^3 binder-treated BCS with a minimal increase in macropores within the 10.0–100.0 μm range, which resulted in a more densely packed BCS matrix. Development of dense BCS pore structure was attributed to the formation of cementitious compounds which filled

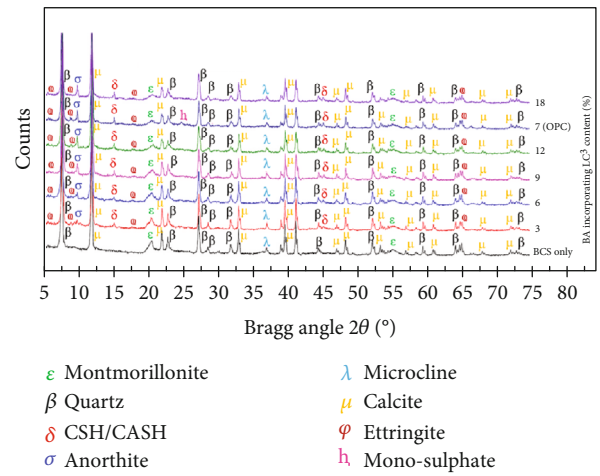

Figure 11: Variations in XRD patterns at various binder contents considering 28 curing days.

micro-macropores and created a denser structure. Besides, Figure 10 portrays the cumulative pore volume (CPV) of untreated and treated BCS with BA incorporating LC^3 binder for specimens cured at 28 days. Typically, Figure 10 demonstrates that the CPV performance of untreated and treated BCS samples poses similar behaviour in performance to PSD behaviour. In other ways, BA incorporating LC^3 binder-based treatment ameliorated the micropore structure of BCS in terms of CPV (Figure 10), as validated by PSD results (Figure 9).

To promote understanding of strength improvement behaviour of BA incorporating LC^3 binder-treated BCS, mineral components of untreated and treated BCS were investigated using XRD analysis for specimens cured at 28 days. Figure 11 depicts XRD patterns showing positions and spacing of atoms for untreated and treated BCS. To

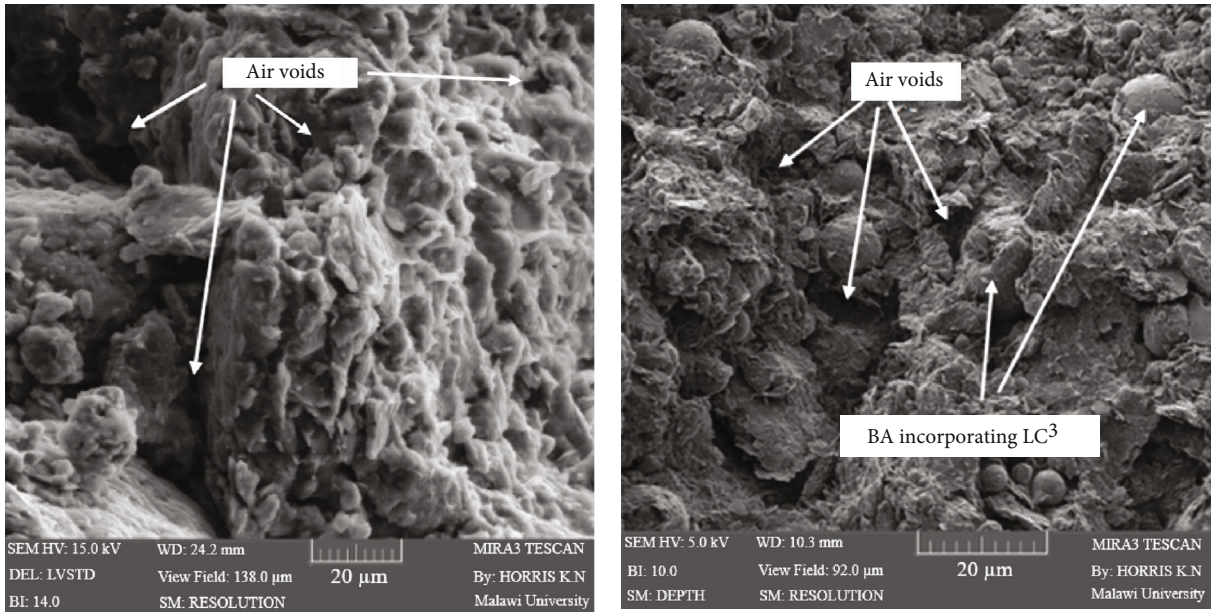

(a) (b)

Figure 12: SEM image at 5 μm for 28 curing days: (a) untreated BCS and (b) treated BCS.

TABLE 5: Mix design of binders for 1.0-ton dry BCS.

Material	BA incorporating LC^3	OPC
BA (kg)	126	—
LC^3 (kg)	84	—
OPC (kg)	—	210

TABLE 6: Basic parameter coefficients of ICF and cost for BA incorporating LC^3 components, materials and OPC material used for BCS stabilisation technique.

Material	ICF (t CO_2/t)	Cost ($/t)
BA	0.101	1.26
Limestone	0.033	32.10
Calcined clay	0.195	43.15
Ground clinker	0.719	149.26
Gypsum	0.120	21.40
OPC	0.907	161.47

illustrate, untreated BCS consisted of montmorillonite peaks. The presence of montmorillonite mineral in untreated BCS validated the high swelling behaviour of this BCS (Figure 2). Whereas with treated BCS specimens, CSH minerals were detected. According to a study by Pacheco et al. [69], CSH minerals result in strength improvement of treated swelling soils. Besides, 7% OPC binder-treated BCS was integrated and exhibited comparable trends of cementitious minerals. Notable variation lay in the formation of monosulphate for OPC binder-treated BCS compared to BA incorporating LC^3 binder-treated BCS. Similar studies by Yoghoubi et al. [70] and Jiang et al. [71] described that the ettringite phase in OPC binder-treated soils tends to be unstable and transforms into monosulphate due to the extinguishing of Gyp contained in OPC. Besides, as further observed in Figure 11, the 2θ peaks of untreated BCS are large, and those of treated BCS are significantly reduced, comparatively. Such a notable peak intensity reduction depicts the ability of BA incorporating LC^3 binder contents to interact with the inner layered montmorillonite structure, resulting in an outstanding decline in peak intensities. Furthermore, the decline in peaks of nonclay minerals such as microcline, calcite and quartz also highlights that the addition of BA incorporating LC^3 binder content effectively reacted and consumed nonclay minerals. This phenomenon resulted in new cementing peaks formation consisting of ettringite and anorthite phases, hence contributing to the improvement of mechanical properties of stabilised BCS [69–71].

To further advance understanding of strength improvement behaviour of BA incorporating LC^3 binder-treated BCS, the microstructure fabric of untreated and BCS treated with 18% BA incorporating LC^3 binder content was evaluated using SEM analysis for cured specimens at 28 days, and results are depicted in Figure 12. As observed in Figure 12, untreated BCS has more microstructural air voids, which are generally large air voids (Figure 12a). However, the microstructure of treated BCS with BA incorporating LC^3 binder shows closely arranged particles with relatively small air voids (Figure 12b). The microstructure of treated BCS demonstrated a densely agglomerated and flocculated arrangement, resulting in the aggregation of BCS particles and a notable decrease in air voids. Moreover, the predominant air voids for treated BCS were smaller ones, indicating a densely packed compact structure and spotlighting the formation of cementitious hydration compounds. Thus, BCS

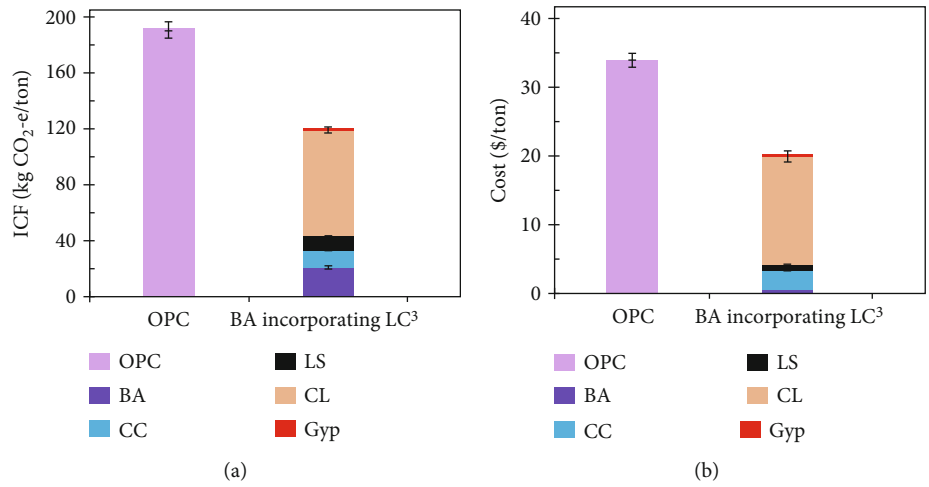

Figure 13: Treated BCS: (a) integrated carbon footprint and (b) cost.

particles were attached to BA incorporating LC^3 binder particles by these formed cementitious compounds. This attachment restrained air voids and led to a denser and more stable structure, thereby increasing the density and strength of treated BCS.

3.7. Ecological and Cost Implications. To assess carbon footprint and costs for BCS treatment with BA incorporating LC^3 binder in this study, 1.0 ton of treated BCS was considered. Carbon footprint and cost estimations were calculated based on comparative analysis to that of treated BCS with traditional OPC binder. The mix design of treating 1.0 ton of BCS with BA incorporating LC^3 binder and OPC binder is given in Table 5.

Ecological assessments were performed using life cycle inventory (LCI) in accordance with ISO 14040 [72]. One parameter, integrated carbon footprint (ICF), was introduced. ICF denotes CO_2 emissions during raw material extraction, transportation and manufacturing [72, 73]. Table 6 presents parameter coefficients of ICF for adopted raw materials based on the ecoinventory database and literature [10–14]. The cost of BA, LC^3 and OPC materials was analysed with regard to the prices of materials in Malawi, converted into US dollars ($).

To extensively evaluate ecological and economical efficiency of mixtures, ICF and cost of mixtures were calculated and compared as presented in Figure 13. BA incorporating LC^3 binder-treated BCS has the smallest values of ICF and cost, indicating 111.51 kgCO_2/ton (Figure 13a) and 19.89 $/ton (Figure 13b), respectively. Compared with OPC binder-treated BCS mixture, ICF and cost of BA incorporating LC^3 binder-treated BCS were reduced by 70.8% (Figure 13a) and 70.5% (Figure 13b), respectively. This shows that BA incorporating LC^3 binder-treated BCS has the most remarkable ecological and economic efficiency, whereas OPC binder-treated BCS has a higher impact on ICF and cost, as also concluded by similar studies [73–75]. Overall, BA incorporating LC^3 binder was recommended as a cleaner promising option for treatment of BCS relevant to road pavement applications.

4. Conclusion

Blended cementitious binder from BA and LC^3 materials was prepared as a cleaner and cost-effective binder for the stabilisation of challenging swelling BCS. Main conclusions were drawn as follows:

1. Stabilisation of BCS using BA incorporating LC^3 binder completely reduced swelling behaviour of treated BCS. The BCS transformed from high swelling behaviour to nonswelling behaviour, complying with requirements for subgrade road pavement applications.

2. BA incorporating LC^3 binder stabilisation improved the mechanical performance of BCS. With the increase in BA incorporating LC^3 binder additive content, the BCS showed significant improvement in MDD and OMC compaction parameters. UCS significantly increased along with curing periods, which implied an increase in BA incorporating LC^3 binder–BCS chemical interactions in water presence, which resulted in formation of cementitious hydration products. Besides, with increase in BA incorporating LC^3 binder dosages to BCS, CBR significantly improved, satisfying requirements for foundation subgrade, subbase and base road pavement constructions.

3. Due to adhesion of cementitious hydration products to BCS particles, shear strength, cohesion and internal friction angle of treated BCS improved with BA incorporating LC^3 binder content and curing period. Shear strength behaviour sheds light on BA incorporating LC^3 binder-treated BCS performance which can help to develop more effective techniques for BCS treatment.

4. PSD, XRD and SEM measurements showed the stabilisation mechanism behind treated BCS samples. Mixing of BCS, BA incorporating LC^3 binder and water

led to pozzolanic reaction and development of cementitious hydration products, which filled BCS air voids, leading to a more dense and stable structure, thereby increasing density and strength of treated BCS.

5. Ecological and cost assessments indicated that utilisation of BA incorporating LC^3 binder in place of OPC for BCS stabilisation can significantly reduce carbon footprint and tremendously reduce BCS stabilisation cost. This is critical to mitigate current climate change challenges in pursuit to achieve sustainability goals Numbers 12 and 13 set by United Nations.

This study has demonstrated that BA incorporating LC^3 binder-treated BCS poses excellent geotechnical performance, which is essential in ensuring reliability and stability of BCS foundations of road projects. However, only FSI, compaction, UCS, CBR-soaked and CD direct shear strength properties, including PSD, XRD and SEM analyses, were investigated. This may not comprehensively mirror treated BCS performance under other geotechnical construction conditions relevant to road applications, such as long-term durability studies under wetting–drying cycles or freezing–thawing cycles, different loading types, curing conditions and temperatures. Thus, future studies may consider more actual geotechnical engineering properties, including durability performance, triaxial shear strength, resilient modulus and permeability studies to fully capture material behaviour under various loading conditions. Future research works may also consider providing quality control procedures for field implementation and performing a rigorous life cycle assessment on BA incorporating LC^3 binder stabilisation of BCS and other soil types using materials sourced from different geographical locations other than Shire Valley in Malawi.

Data Availability Statement

This article includes the data used to support the findings.

Conflicts of Interest

The authors declare no conflicts of interest.

Funding

No funding was received for this manuscript.

References

[1] A. Maneli, W. K. Kupolati, O. S. Abiola, and J. M. Ndambuki, "Influence of Fly Ash, Ground-Granulated Blast Furnace Slag and Lime on Unconfined Compressive Strength of Black Cotton Soil," *Road Materials and Pavement Design* 17, no. 1 (2016): 252–260, https://doi.org/10.1080/14680629.2015.1066703.

[2] S. Patel and J. T. Shahu, "Engineering Properties of Black Cotton Soil–Dolime Mix for Its Use as Subbase Material in Pavements," *International Journal of Geomate* 8, no. 1 (2015): 1159–1166, https://doi.org/10.21660/2015.15.4191.

[3] B. A. Chethan and A. U. R. Shankar, "Strength and Durability Characteristics of Cement and Class F Fly Ash-Treated Black Cotton Soil," *Indian Geotechnical Journal* 51, no. 5 (2021): 1121–1133, https://doi.org/10.1007/s40098-020-00488-2.

[4] P. K. Amrutha, K. S. Muthu, V. B. Vaishnavi, S. S. Mahesh, and P. Aavani, "Black Cotton Soil Stabilization Using Bagasse Ash and Lime," *International Journal of Civil Engineering and Technology (IJCIET)* 67, no. 6 (2016): 460–471.

[5] M. J. Aliyu, L. Z. Adam, and S. U. Kunya, "Investigating the Engineering Properties of Black Cotton Soil Treated With Rice Husk Ash," *African Scholar Journal of Env. Design & Construction Mgt* 18, no. 4 (2020).

[6] S. Himani, J. Kitendra, and A. Biswajit, "Stabilization of Black Cotton Soil by Using Sugarcane Bagasse Ash," *International Journal of Scientific Research and Review* 7, no. 1 (2019).

[7] L. A. Sofri, M. Abdullah, A. V. Sandu, et al., "Mechanical Performance of Fly Ash Based Geopolymer (FAG) as Road Base Stabilizer," *Materials* 15, no. 20 (2022): 7242, https://doi.org/10.3390/ma15207242.

[8] P. Ghadira and N. Ranjbar, "Clayey Soil Stabilization Using Geopolymer and Portland Cement," *Construction and Building Materials* 188 (2018): 361–371, https://doi.org/10.1016/j.conbuildmat.2018.07.207.

[9] Y. Izumi, A. Iizuka, and H. J. Ho, "Calculation of Greenhouse Gas Emissions for a Carbon Recycling System Using Mineral Carbon Capture and Utilization Technology in the Cement Industry," *Journal of Cleaner Production* 312 (2021): 127618, https://doi.org/10.1016/j.jclepro.2021.127618.

[10] N. Mohamad, K. Muthusamy, R. Embong, A. Kusbiantoro, and M. H. Hashim, "Environmental Impact of Cement Production and Solutions: A Review," *Materials Today Proceedings* 48 (2022): 741–746, https://doi.org/10.1016/j.matpr.2021.02.212.

[11] K. L. Scrivener, V. M. John, and E. M. Gartner, "Eco-Efficient Cements: Potential Economically Viable Solutions for a Low-CO2 Cement Based Materials Industry," *Cement and Concrete Research* 114 (2018): 2–26, https://doi.org/10.1016/j.cemconres.2018.03.015.

[12] D. N. Huntzinger and T. D. Eatmon, "A Life-Cycle Assessment of Portland Cement Manufacturing: Comparing the Traditional Process With Alternative Technologies," *Journal of Cleaner Production* 17, no. 7 (2009): 668–675, https://doi.org/10.1016/j.jclepro.2008.04.007.

[13] B. C. McLellan, R. P. Williams, J. Lay, A. V. Riessen, and G. D. Corder, "Costs and Carbon Emissions for Geopolymer Pastes in Comparison to Ordinary Portland Cement," *Journal of Cleaner Production* 19, no. 9-10 (2011): 1080–1090, https://doi.org/10.1016/j.jclepro.2011.02.010.

[14] C. Shi, A. F. Jiménez, and A. Palomo, "New Cements for the 21st Century: The Pursuit of an Alternative to Portland Cement," *Cement and Concrete Research* 41, no. 7 (2011): 750–763, https://doi.org/10.1016/j.cemconres.2011.03.016.

[15] M. S. Imbabi, C. Carrigan, and S. McKenna, "Trends and Developments in Green Cement and Concrete Technology," *International Journal of Sustainable Built Environment* 1, no. 2 (2012): 194–216, https://doi.org/10.1016/j.ijsbe.2013.05.001.

[16] P. Saingam, B. Chatveera, P. Promsawat, et al., "Synergizing Portland Cement, High-Volume Fly Ash and Calcined Calcium Carbonate in Producing Self-Compacting Concrete: A Comprehensive Investigation of Rheological, Mechanical, and Microstructural Properties," *Case Studies in Construction Materials* 21 (2024): e03832, https://doi.org/10.1016/j.cscm.2024.e03832.

[17] N. Wongvatana, A. Noorak, P. Jongpradist, and P. Jamsawang, "Geotechnical Performance and Environmental Assessment of Eucalyptus Wood Ash–Stabilized Sediment for Pavement Infrastructure," *Transportation Infrastructure Geotechnology* 12, no. 5 (2025): https://doi.org/10.1007/s40515-025-00600-0.

[18] P. Jamsawang, H. Poorahong, P. Jongpradist, S. Likitlersuang, and S. Chaiyaput, "Destructive and Nondestructive Characteristics of Solidified Reservoir Sediments Incorporating Microstructural Analyses," *Bulletin of Engineering Geology and the Environment* 81, no. 8 (2022): https://doi.org/10.1007/s10064-022-02797-7.

[19] M. Jamnongwong, N. Wongvatana, A. Noorak, P. Jongpradist, S. Chaiprakaikeow, and P. Jamsawang, "Mechanical and Environmental Performance of Cement-Eucalyptus Ash Stabilized Dam Sediments for Sustainable Road Construction," *International Journal of Geosynthetics and Ground Engineering* 11, no. 3 (2025): https://doi.org/10.1007/s40891-025-00637-8.

[20] H. Abdullah, M. A. Shahin, and P. Sarker, "Use of Fly-Ash Geopolymer Incorporating Ground Granulated Slag for Stabilisation of Kaolin Clay Cured at Ambient Temperature," *Geotechnical and Geological Engineering* 37, no. 2 (2019): 721–740, https://doi.org/10.1007/s10706-018-0644-2.

[21] D. Petersen, R. Link, N. Pandian, and K. Krishna, "The Pozzolanic Effect of Fly Ash on the California Bearing Ratio Behavior of Black Cotton Soil," *Journal of Testing and Evaluation* 31 (2003).

[22] N. Wongvatana, S. Lhajai, H. Poorahong, P. Jongpradist, and P. Jamsawang, "Performance, Environmental Impact, and Cost Evaluation of Eucalyptus Ash-Stabilised Dam Sediments for Sustainable Pavement Engineering," *International Journal of Pavement Engineering* 26, no. 1 (2025): https://doi.org/10.1080/10298436.2025.2520028.

[23] N. Wongvatana, A. Noorak, H. Poorahong, P. Jongpradist, S. Chaiprakaikeow, and P. Jamsawang, "Sustainable-Road Construction Materials Incorporating Dam Sediment and Eucalyptus Ash Waste: A Circular Economy Framework," *Case Studies in Construction Materials* 22 (2025): e04118, https://doi.org/10.1016/j.cscm.2024.e04118.

[24] S. Farhan Mushtaq, A. Ali, R. A. Khushnood, et al., "Effect of Bentonite as Partial Replacement of Cement on Residual Properties of Concrete Exposed to Elevated Temperatures," *Sustainability* 14, no. 18 (2022): 11580, https://doi.org/10.3390/su141811580.

[25] G. Habert, J. B. D. E. De Lacaillerie, and N. Roussel, "An Environmental Evaluation of Geopolymer Based Concrete Production: Reviewing Current Research Trends," *Journal of Cleaner Production* 19, no. 11 (2011): 1229–1238, https://doi.org/10.1016/j.jclepro.2011.03.012.

[26] I. Kafodya, D. Basuroy, J. M. Marangu, G. Kululanga, R. Maddalena, and V. I. Novelli, "Mechanical Performance and Physico-Chemical Properties of Limestone Calcined Clay Cement (LC3) in Malawi," *Buildings* 13, no. 3 (2023): 740, https://doi.org/10.3390/buildings13030740.

[27] N. Wu, T. Ji, P. Huang, T. Fu, X. Zheng, and Q. Xu, "Use of Sugar Cane Bagasse Ash in Ultra-High-Performance Concrete (UHPC) as Cement Replacement," *Construction and Building Materials* 317 (2022): 125881, https://doi.org/10.1016/j.conbuildmat.2021.125881.

[28] V. Jittin, S. N. Minnu, and A. Bahurudeen, "Potential of Sugarcane Bagasse Ash as Supplementary Cementitious Material and Comparison With Currently Used Rice Husk Ash," *Construction and Building Materials* 273 (2021): 121679, https://doi.org/10.1016/j.conbuildmat.2020.121679.

[29] G. Sua-Iam and N. Makul, "Use of Increasing Amounts of Bagasse Ash Waste to Produce Self-Compacting Concrete by Adding Limestone Powder Waste," *Journal of Cleaner Production* 57 (2013): 308–319, https://doi.org/10.1016/j.jclepro.2013.06.009.

[30] N. H. Serker, R. U. Hafiz, A. H. Rahman, and M. Ashikuzzaman, "Suitability of Using Sugarcane Bagasse Ash as Partial Replacement of Cement in Concrete," in *5th International Conference on Advances in Civil Engineering* (CUET, 2020).

[31] P. Chindaprasirt, P. Sujumnongtokul, and P. Posi, "Durability and Mechanical Properties of Pavement Concrete Containing Bagasse Ash," *Materials Today: Proceedings* 17 (2019): 1612–1626, https://doi.org/10.1016/j.matpr.2019.06.191.

[32] A. Bahurudeen, D. Kanraj, V. Gokul Dev, and M. Santhanam, "Performance Evaluation of Sugarcane Bagasse Ash Blended Cement in Concrete," *Cement and Concrete Composites* 59 (2015): 77–88, https://doi.org/10.1016/j.cemconcomp.2015.03.004.

[33] J. Bajaj and V. K. Singh, "Performance Evaluation of Black Cotton Soil Stabilized With Sugarcane Bagasse Ash and Randomly Distributed Coir Fibres," *International Journal for Innovative Research in Science & Technology* 2, no. 11 (2016): 493–498.

[34] T. Sharma and R. Kaushik, "Effect of Polypropylene Fiber on Properties of Bagasse Ash-Cement Stabilized Clay Soil," *International Journal on Emerging Technologies* 10, no. 2 (2019): 255–266.

[35] H. Hasan, L. Dang, H. Khabbaz, B. Fatahi, and S. Terzaghi, "Remediation of Expansive Soils Using Agricultural Waste Bagasse Ash," *Procedia Engineering* 143 (2016): 1368–1375, https://doi.org/10.1016/j.proeng.2016.06.161.

[36] Y. C. Díaz, S. S. Berriel, U. Heierli, et al., "Limestone Calcined Clay Cement as a Low-Carbon Solution to Meet Expanding Cement Demand in Emerging Economies," *Development Engineering* 2 (2017): 82–91, https://doi.org/10.1016/j.deveng.2017.06.001.

[37] K. Scrivener, F. Martirena, S. Bishnoi, and S. Maity, "Calcined Clay Limestone Cements (LC^3)," *Cement and Concrete Research* 114 (2018): 49–56, https://doi.org/10.1016/j.cemconres.2017.08.017.

[38] A. Akindahunsi, F. Avet, and K. Scrivener, "The Influence of Some Calcined Clays From Nigeria as Clinker Substitute in Cementitious Systems," *Case Studies in Construction Materials* 13 (2020): e00443, https://doi.org/10.1016/j.cscm.2020.e00443.

[39] S. Joseph, S. Bishnoi, and S. Maity, "An Economic Analysis of the Production of Limestone Calcined Clay Cement in India," *Indian Concrete Journal* 90, no. 11 (2016): 22–27.

[40] N. Ijaz, W. M. Ye, Z. ur Rehman, Z. Ijaz, and M. F. Junaid, "Global Insights Into Micro-Macro Mechanisms and Environmental Implications of Limestone Calcined Clay Cement (LC3) for Sustainable Construction Applications," *Science of the Total Environment* 907 (2024): 167794, https://doi.org/10.1016/j.scitotenv.2023.167794.

[41] M. D. Sheikh, T. Jamil, T. Ayub, A. U. R. Khan, S. M. Bilal, and C. Hu, "Comparative Study on LC^3-50 With OPC Concrete Using Raw Materials From Pakistan," *Advances in Materials Science and Engineering* 2023 (2023): 5503670, https://doi.org/10.1155/2023/5503670.

[42] M. Sharma, S. Bishnoi, F. Martirena, and K. Scrivener, "Limestone Calcined Clay Cement and Concrete: A State-of-the-Art Review," *Cement and Concrete Research* 149 (2021): 106564, https://doi.org/10.1016/j.cemconres.2021.106564.

[43] J. Wang, D. Shi, Y. Xia, et al., "Stabilization/Solidification of Radioactive Borate Waste via Low-Carbon Limestone Calcined Clay Cement (LC^3)," *Journal of Environmental Chemical Engineering* 12, no. 3 (2024): 113129, https://doi.org/10.1016/j.jece.2024.113129.

[44] V. A. Reddy, C. H. Solanki, S. Kumar, K. R. Reddy, and Y. J. Du, "New Ternary Blend Limestone Calcined Clay Cement for Solidification/Stabilization of Zinc Contaminated Soil," *Chemosphere* 235 (2019): 308–315, https://doi.org/10.1016/j.chemosphere.2019.06.051.

[45] I. Wilińska, P. Barbara, and A. Ostrowski, "Investigation of Different Ways of Activation of Fly Ash–Cement Mixtures: Part 2 - Mechanical Activation," *Journal of Thermal Analysis and Calorimetry* 149, no. 20 (2024): 11389–11406, https://doi.org/10.1007/s10973-023-12503-8.

[46] A. O. Eberemu, "Evaluation of Bagasse Ash Treated Lateritic Soil as a Potential Barrier Material in Waste Containment Application," *Acta Geotechnica* 8, no. 4 (2013): 407–421, https://doi.org/10.1007/s11440-012-0204-5.

[47] ASTM D2216-17, *Standard Test Method for Laboratory Determination of Water (Moisture) Content of Soil and Rock by Mass* (ASTM, 2017).

[48] ASTM D854-23, *Standard Test Methods for Specific Gravity of Soil Solids by Water Displacement Method* (ASTM, 2023).

[49] ASTM D4318-17, *Standard Test Methods for Liquid Limit, Plastic Limit, and Plasticity Index of Soils* (ASTM, 2018).

[50] ASTM D6913-04, *Standard Test Methods for Particle Size Distribution (Gradation) of Soils Using Sieve Analysis* (ASTM, 2009).

[51] ASTM C618-08, *Standard Specification for Coal Fly Ash and Raw or Calcined Natural Pozzolan for Use in Concrete* (Annual Book of ASTM Standards, 2008).

[52] ASTM C150-07, *Standard Specification for Portland Cement* (ASTM, 2007).

[53] H. K. Nangulama and S. P. Rimoy, "Feasibility of Using Bagasse Ash Incorporating Limestone Calcined Clay Cement as Ordinary Portland Cement Replacement for Stabilisation of Black Cotton Soils," *Cleaner Waste Systems* 10 (2025): 100226, https://doi.org/10.1016/j.clwas.2025.100226.

[54] H. K. Nangulama and S. Rimoy, "Effectiveness of Bagasse Ash Incorporating Limestone Calcined Clay Cement (LC^3) in Improving Shear Strength and Durability Properties of Black Cotton Soils," *Advances in Civil Engineering* 2024 (2024): 7112465, https://doi.org/10.1155/adce/7112465.

[55] BS EN 12390, *Testing Hardened Concrete: Compressive Strength of Test Specimens* (British Standards, 2009).

[56] BS EN 197-1, *Composition, Specifications and Conformity Criteria for Common Cements* (BSI, 2011).

[57] BS EN 413-1, *Masonry Cement Composition, Specification and Conformity Criteria* (BSI, 2011).

[58] ASTM D698-12, "Standard Test Methods for Laboratory Compaction Characteristics of Soil Using Standard Effort," *ASTM International* 3 (2012): 1–13.

[59] ASTM D4829-21, *Standard Test Method for Expansion Index of Soils* (ASTM, 2021).

[60] ASTM D2166, *Standard Test Method for Unconfined Compressive Strength of Cohesive Soils* (ASTM, 2010).

[61] ASTM D1883-16, *Standard Test Method for California Bearing Ratio (CBR) of Laboratory-Compacted Soils* (ASTM International, 2016).

[62] ASTM D3080, "Standard Test Method for Direct Shear Test of Soils Under Consolidated Drained Conditions," ASTM International, 2011).

[63] MMW, *Volume III: Pavements and Materials Design; Highway Manual Part 1* (Malawi Ministry of Works, 2015).

[64] Indian Roads Congress, "Guidelines for Soil and Granular Material Stabilization Using Cement, Lime and Fly Ash," *Indian Roads Congress* 89 (2010): 1–37.

[65] T. Nagaraj and N . Miura, *Soft Clay Behaviour Analysis and Assessment* (CRC Press, 2021).

[66] K. Kasama, K. Zen, and K. Iwataki, "Undrained Shear Strength of Cement Treated Soils," *Soils and Foundations* 46, no. 2 (2006): 221–232, https://doi.org/10.3208/sandf.46.221.

[67] U. Calik and E. Sadoglu, "Classification, Shear Strength, and Durability of Expansive Clayey Soil Stabilized With Lime and Perlite," *Natural Hazards* 71, no. 3 (2014): 1289–1303, https://doi.org/10.1007/s11069-013-0950-1.

[68] X. Kang, L. Ge, and W. C. Liao, "Cement Hydration-Based Micromechanics Modeling of the Time-Dependent Small-Strain Stiffness of Fly Ash-Stabilized Soils," *International Journal of Geomechanics* 16, no. 3 (2016): https://doi.org/10.1061/(ASCE)GM.1943-5622.0000552.

[69] T. F. Pacheco-Torgal, J. Castro-Gomes, and S. Jalali, "Alkali-Activated Binders: A Review: Part 1. Historical Background, Terminology, Reaction Mechanisms and Hydration Products," *Construction and Building Materials* 22, no. 7 (2008): 1305–1314, https://doi.org/10.1016/j.conbuildmat.2007.10.015.

[70] M. Yaghoubi, A. Arulrajah, M. M. Disfani, S. Horpibulsuk, M. W. Bo, and S. Darmawan, "Effects of Industrial By-Product Based Geopolymers on the Strength Development of a Soft Soil," *Soils and Foundations* 58, no. 3 (2018): 716–728, https://doi.org/10.1016/j.sandf.2018.03.005.

[71] N. Jiang, Y. J. Du, S. Liu, M. L. Wei, S. Horpibulsuk, and A. Arulrajah, "Multi-Scale Laboratory Evaluation of the Physical, Mechanical and Microstructural Properties of Soft Highway Subgrade Soil Stabilized With Calcium Carbide Residue," *Canadian Geotechnical Journal* 53, no. 3 (2015): 373–383.

[72] ISO 14040, "Environmental Management – Life Cycle Assessment – Principles and Framework," International Organisation for Standardisation, 2006).

[73] J. Yu, H. L. Wu, D. K. Mishra, G. Li, and C. K. Y. Leung, "Compressive Strength and Environmental Impact of Sustainable Blended Cement With High-Dosage Limestone and Calcined Clay (LC2)," *Journal of Cleaner Production* 278 (2021): 123616, https://doi.org/10.1016/j.jclepro.2020.123616.

[74] C. Kulasuriya, V. Vimonsatit, and W. P. S. Dias, "Performance Based Energy, Ecological and Financial Costs of a Sustainable Alternative Cement," *Journal of Cleaner Production* 287 (2021): 125035, https://doi.org/10.1016/j.jclepro.2020.125035.

[75] I. Faridmehr, M. L. Nehdi, M. Nikoo, G. F. Huseien, and T. Ozbakkaloglu, "Life-Cycle Assessment of Alkali-Activated Materials Incorporating Industrial Byproducts," *Materials* 14, no. 9 (2021): 2401, https://doi.org/10.3390/ma14092401.